**Supplementary figure 1**

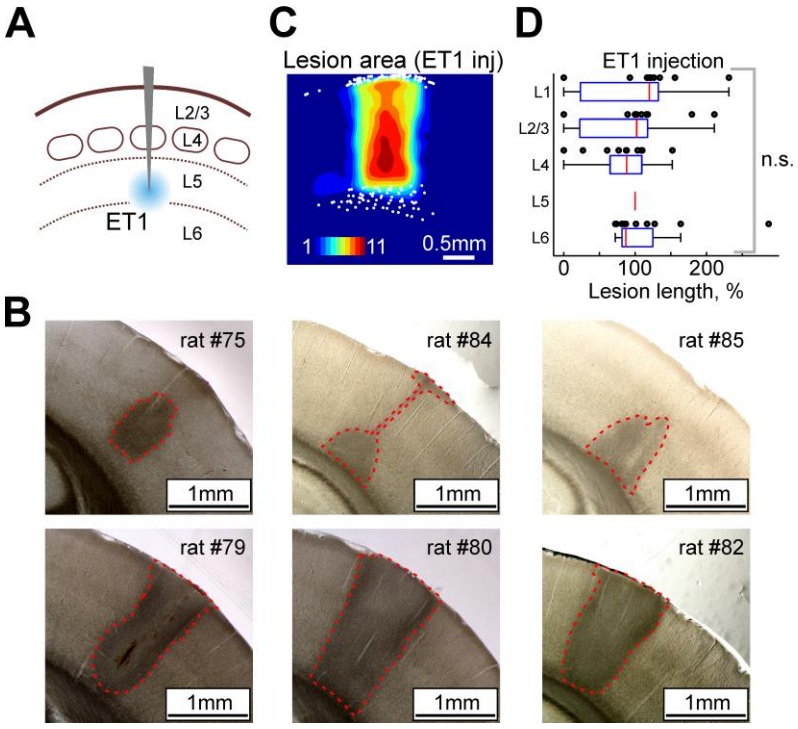


**Supplementary figure 1. Ischemic lesions formed after intracortical ET1 injection into deep layers of the rat barrel cortex.**

**(A)** ET1 (1μM, 1-3 μl) is injected into infragranular layer of barrel cortex at depth 1000-1200 μm. **(B)** Examples of coronal brain slices with spherical- (top row) and pillar- (bottom row) shape ischemic foci formed 3 hours after ET1 injection into deep layers. The borders of lesions are marked by dashed red lines. **(C)** Cumulative probability image of the ischemic lesion formed 3 hours after ET1 exposure, obtained by superimposing the lesion areas. White dots indicate cortical boundaries. **(D)** Lesion length in cortical layers normalized to the lesion length in L5. C-D: pooled data from 11 rats.

**Supplementary figure 2**

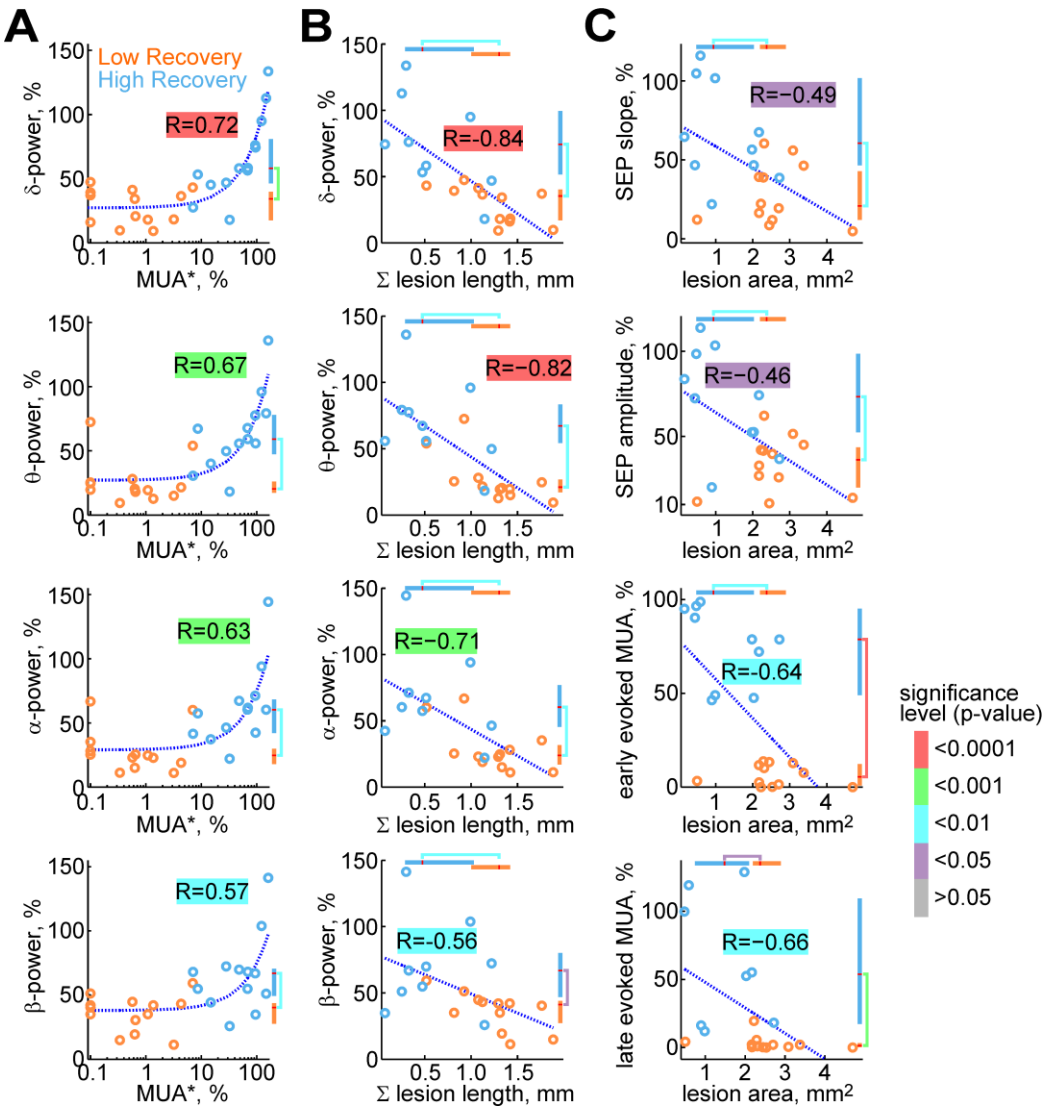


**Supplementary figure 2. Correlation of the electrical activity depression with a degree of ischemic damage.**

**(A)** Spontaneous FP power averaged over layers versus MUA*. **(B)** Spontaneous FP power averaged over layers versus sum of linear size of ischemic focus in four layers (L2/3, L4, L5 and L6). FP power in delta-, theta-, alpha- and beta- frequency bands after 3h of ET1 wash out was normalized to control values. **(C)** Parameters of evoked activity versus area of ischemic focus on axial slice. SEP slope, SEP amplitude, early and late evoked MUA after 3h of ET1 wash out was normalized to control values.

**Supplementary figure 3**

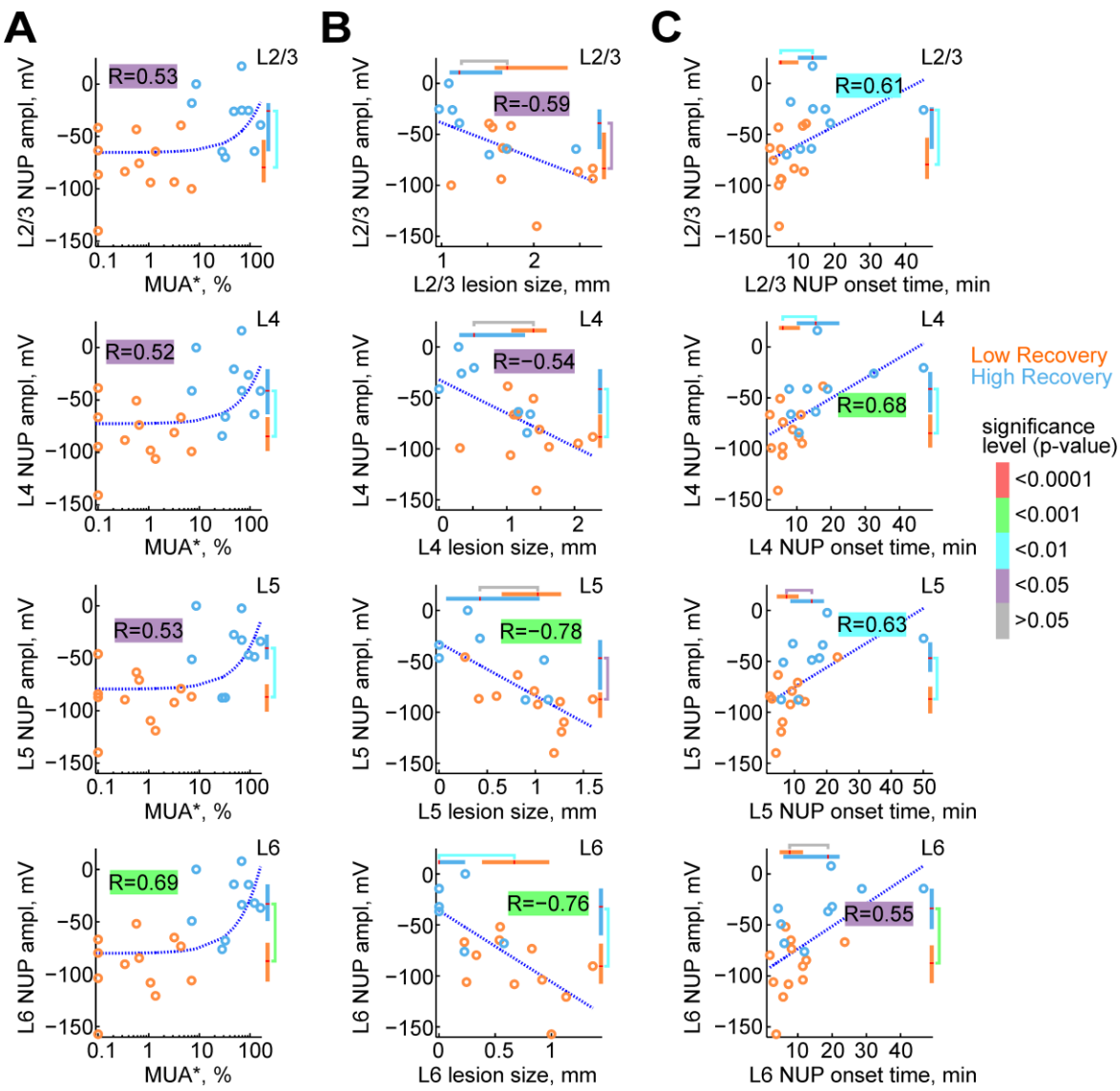


**Supplementary figure 3. Correlation of NUPs with a degree of ischemic damage.**

**(A)** Dependence of negative ultraslow potential (NUP) amplitude on MUA* in different layers of the cortex. The amplitude of NUP was calculated as difference of potential level on a NUP peak and potential in control period. **(B)** Dependence of NUP amplitude on characteristic linear size of ischemic focus in different cortical layers. **(C)** Dependence of NUP amplitude on NUP onset in different cortical layers.

**Supplementary figure 4**

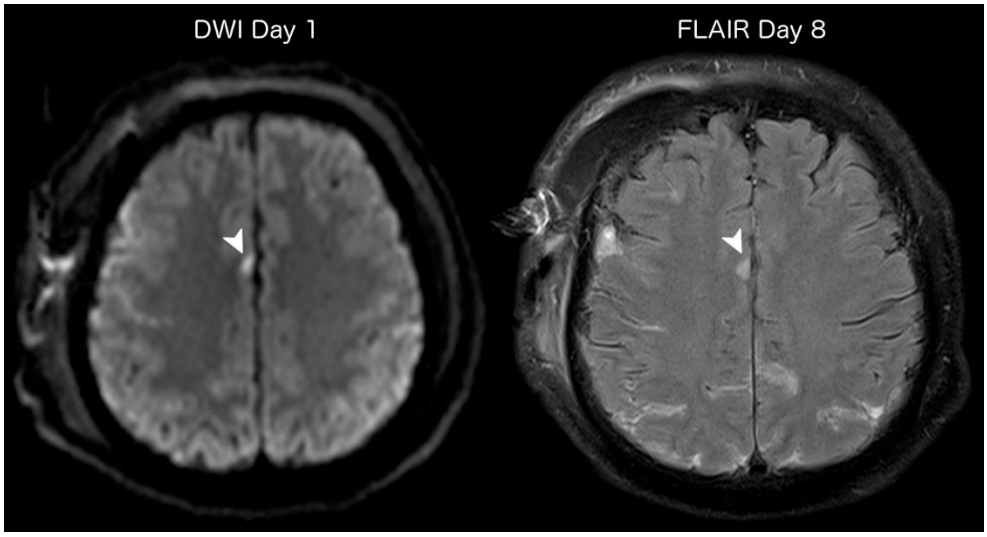


**Supplementary figure 4.** Representative MR images of a 57-year-old male patient with grade four aneurysmal subarachnoid hemorrhage (aSAH) according to the modified Fisher scale from an anterior communicating artery aneurysm. The patient was enrolled at Charité – Universitätsmedizin Berlin in the prospective, observational, multicenter, cohort, diagnostic phase III trial 'Depolarizations in ischemia after subARachnoid hemorrhaGE-1' (Dreier et al. 2022). MRI examinations were performed on a 1.5 T scanner. Diffusion weighted image (DWI) of the first postoperative MRI on day one showed a linear hyperintensity in the right frontomedial cortex (arrowhead). The corresponding fluid-attenuation inversion recovery (FLAIR) image was without abnormal findings. However, FLAIR imaging on day eight then showed a wedge-shaped hyperintensity with a base measuring ten mm at the surface of the cortex (arrowhead). These findings are consistent with a small cortical infarct at the interhemispheric fissure that developed early after aSAH. Wedge-shaped infarcts after aSAH are known from human autopsies and the primate model of aSAH (Stoltenburg-Didinger and Schwarz 1987; Neil-Dwyer et al. 1994; Schatlo et al. 2010). The wedge base usually extends less than one mm within the cortex, which is below the spatial resolution of a clinical MRI scanner. Overall, the cortical infarct resembles the described histologic infarcts by its wedge shape, but it is ten times larger than the typical histologic counterpart.

**Supplementary figure 5**

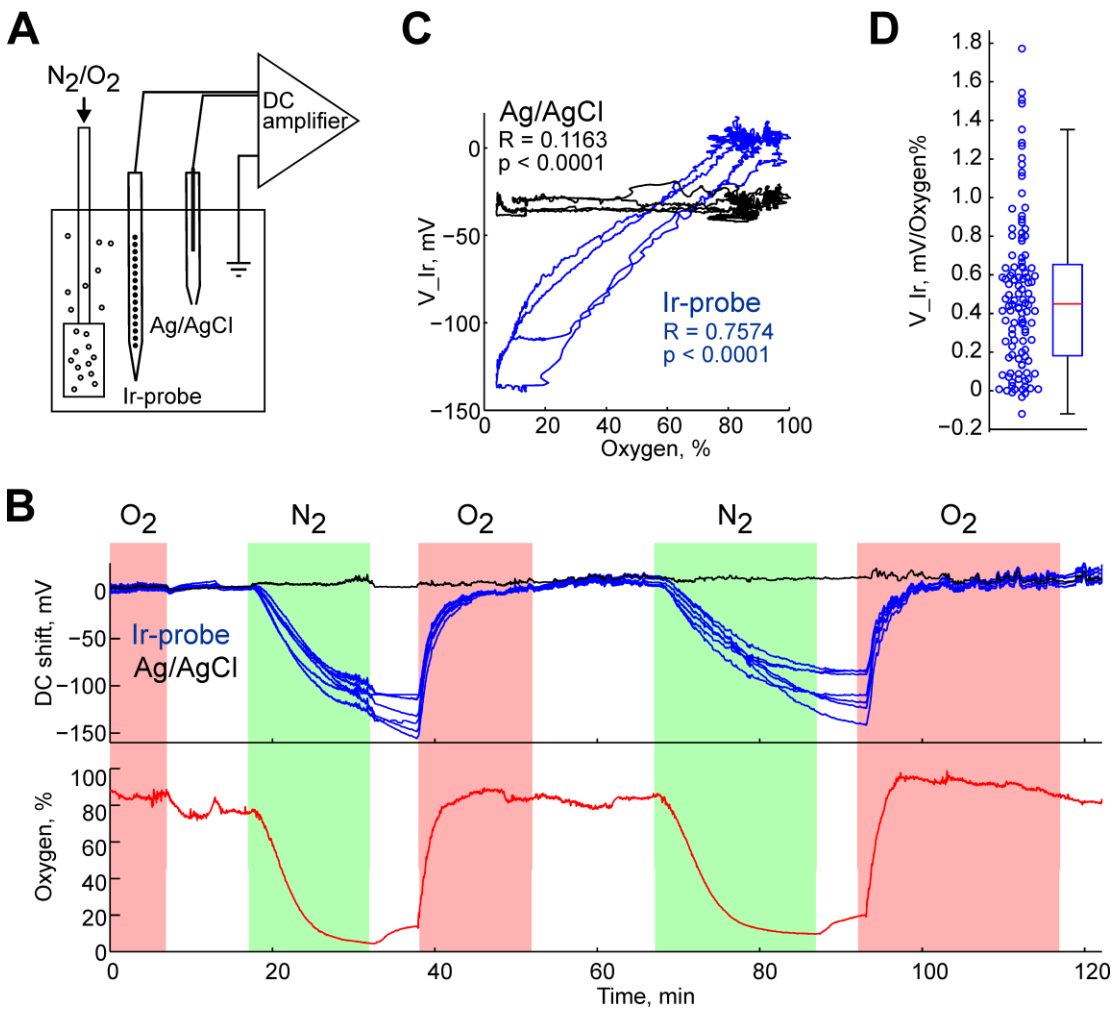


**Supplementary figure 5. Oxygen sensitivity of Iridium electrodes.**

**(A)** Experimental setup. Iridium electrode arrays were immersed in a chamber perfused with artificial cerebrospinal fluid (ACSF). Additional Ag/AgCl electrode was placed in ACSF-filled glass pipette. $pO_2$ was modified by exchanging perfusion from ACSF saturated with 95% $O_2$/ 5% $CO_2$ to ACSF saturated with 95% $N_2$/ 5% $CO_2$. **(B)** Example recordings of voltage responses evoked by $pO_2$ changes in Iridium (blue traces) and Ag/AgCl (black trace) electrodes. Red traces below show $pO_2$ measured with $pO_2$ – sensitive electrodes. **(C)** $pO_2$ – dependence of voltage on one of Iridium and Ag/AgCl electrodes. **(D)** Group data on $pO_2$ – sensitivity of Ir electrodes. Pooled data from 112 Iridium electrodes.